Chemical Engineering and Processing 65 (2013) 58–67

Contents lists available at SciVerse ScienceDirect

Chemical Engineering and Processing: Process Intensification

journal homepage: www.elsevier.com/locate/cep

Near critical and supercritical fluid extraction of Cu(II) from aqueous solutions using a hollow fiber contactor

Hugo Valdés[a,d], Rossana Sepúlveda[a], Julio Romero[a,*], Fernando Valenzuela[b], José Sánchez[c]

[a] Laboratory of Membrane Separation Processes (LabProSeM), Department of Chemical Engineering, University of Santiago de Chile (USACH), Chile
[b] Department of Food Science and Chemical Technology, Faculty of Chemical and Pharmaceutical Sciences, University of Chile (UCH), Chile
[c] Institut Européen des Membranes (UMR 5635 CNRS/UM2/ENSCM), Montpellier, France
[d] School of Construction Engineering, Faculty of Engineering Science, Catholic University of Maule (UCM), Talca, Chile

ARTICLE INFO

Article history:
Received 20 August 2012
Received in revised form
13 December 2012
Accepted 16 December 2012
Available online 22 December 2012

ABSTRACT

The aim of this work is the experimental and theoretical characterization of the mass transfer in a membrane-based dense gas extraction of metal ions from aqueous solutions using a hollow fiber contactor. Extractions of Cu(II) were conducted in a single fiber membrane contactor operating under steady state conditions. Aqueous $CuSO_4$ solutions were treated using a CO_2 phase containing 1,1,1-trifluoro-2,4-pentanedione (TFA) or 1,1,1,5,5,5-hexafluoro-2,4-pentanedione (HFA) at 40 °C and pressures ranged between 70 and 90 bar.

Experiments show that the use of dense CO_2 as extraction solvent of Cu(II) ions reaches extraction efficiencies valued up to 98.7%. Simultaneously, a mass transfer model was proposed correlating an effective rate function of the complex formation at the aqueous-CO_2 interface.

The highest extraction efficiencies were observed at higher pressures and lower pH values, which could confirm that a high content of protons is required to facilitate and stabilize the formation complex by means of keto-enol tautomerism.

This work represents the first step in order to propose a novel intensified operation, which could be applied for high valued metals or hazardous materials.

1. Introduction

There is an immense body of literature on solvent extraction of metals using organic solvents, considering that solvent extraction is a relatively new technology compared to other unit operations such as distillation and absorption. A surge in interest in solvent extraction occurred during the 1940s, initiated by its application for uranium production and for reprocessing of irradiated nuclear materials. This first application became a stimulus for the non-nuclear industry and solvent extraction was introduced as separation and purification process in numerous chemical and metallurgical industries in the 1950s and early 1960s. Subsequently, in the 1980s and 1990s, a significant number of studies have been reported in the literature on supercritical fluid (SCF) extraction of a wide variety of matrices with the objective of replacing commercially available organic solvents. Nevertheless, the knowledge developed in the last six decades the studies about SCF extraction of metals from aqueous solutions are relatively few [1–5], and further investigations in this field are necessary to lead to commercial processes using dense carbon dioxide in a wide variety of industries dealing with metals.

The extraction of metals based on a membrane contactor system with conventional solvents is a process widely studied using different configurations, extractants and extraction solvents [6–9]. Generally, several authors [9,10] report studies of extracting metals from aqueous solutions by means of conventional organic solvents such as hexane or kerosene, and commercial extractants, similar to those used in SX extraction.

Here the extraction of Cu^{2+} from aqueous solutions by means of dense gas extraction was achieved by using a hollow fiber membrane contactor device. This application could be described by means of the same phenomenological and thermodynamic principles of conventional contactor operations. Nevertheless, to our knowledge no previous study is available relating to dense gas extraction of metals from aqueous solutions using a membrane contactor operation.

* Corresponding author at: University of Santiago de Chile (USACH), Department of Chemical Engineering, Av. Lib. Bdo. O'Higgins 3363, Estación Central, Santiago, Chile. Tel.: +56 2 718 18 21.
E-mail address: julio.romero@usach.cl (J. Romero).

0255-2701/$ – see front matter © 2012 Elsevier B.V. All rights reserved.
http://dx.doi.org/10.1016/j.cep.2012.12.005

Nomenclature

C	concentration (mol kg^{-1})
D	diffusion coefficient (m^2 s^{-1})
d	diameter (m)
e	membrane thickness (m)
J	flux of Cu^{2+} (mol m^{-2} s^{-1})
K	mass transfer coefficient in boundary layer (m s^{-1})
k_{eff}	kinetic coefficient (mol$^{1-\alpha-\beta}$ s^{-1} m$^{3(\alpha+\beta)}$)
L	length (m)
N	mass transfer flow of Cu^{2+} (mol s^{-1})
P	pressure (Pa)
Re	Reynolds number
S	surface area available for mass transfer (m^2)
Sc	Schmidt number
Sh	Sherwood number
T	temperature (K)
z	stoichiometric ratio

Greek letters

ε	porosity
τ	tortuosity
η	viscosity (kg m^{-1} s^{-1})
μ	dipole moment (Debyes)

Subscripts and superscripts

(1)	refers to aqueous solution boundary layer
(2)	refers to aqueous-dense gas interface
(3)	refers to membrane pores
(4)	refers to dense gas boundary layer
A	refers to extractant
l	refers to liquid
M	refers to metal ion
i	liquid–dense gas interface
0	bulk
eq	refers to equivalent diameter of the shell
C	critical point
R	reduced variable
ID	inner diameter
OD	outer diameter
SL	saturated liquid
VP	vapor
p	pore

2. Membrane-based supercritical fluid extraction of metal ions

2.1. Supercritical fluids and membrane contactors

Although membrane contactor processes can be conducted using a number of different types of module geometry, including flat sheet, spiral wound, rotating annular and hollow fiber, this latter one receives the most attention, since it shows high specific contact surface area per volume (m^2/m^3). Hollow fiber modules targeted for industrial applications (as opposed to medical ones, e.g., blood oxygenation) are available from a variety of sources, although some are designed for pressure-driven filtration processes rather than concentration-driven mass transfer. The most well-known hollow fiber contactor (HFC) module designed for concentration-driven mass transfer is the Liqui-Cel® Extra-Flow module offered by CELGARD LLC [11–13].

The PoroCrit® process or porocritical extraction [14,15] is a commercial SFC extraction which uses a hollow fiber membrane contactor. In this process a macroporous membrane allows the contact between two phases. On one side, an aqueous liquid solution is circulated and on the opposite side the extraction solvent is a near-critical or supercritical fluid. When the membrane used is hydrophobic, the aqueous solution does not penetrate within the membrane porosity. A meniscus is formed in the pore mouth establishing a dense gas–liquid interface. The driving force of the mass transfer process through the membrane is a concentration gradient between both circulating phases. In this operation, permeability and selectivity are defined by the transport phenomena at the proximities and through the membrane coupled to the phase equilibrium between the aqueous feed solution and the CO_2 phase.

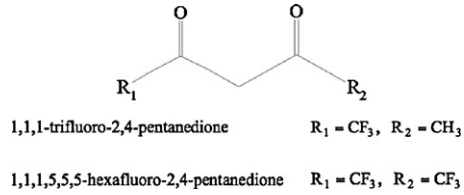

Fig. 1. Chemical structure of extractants used in this study.

The size and number of fibers in a membrane contactor will be determined by the volume of the liquid to be treated. Previous studies on membrane-based dense gas extraction report higher extraction efficiencies when the near critical or supercritical solvent is circulated outside the fibers and the liquid feed solution is circulated in the lumenside [16–18]. This process involves several advantages compared to conventional contactor devices used in supercritical fluid extraction like conventional contacting columns that disperse one fluid phase in another. In this case, the modularity of this membrane contactor application is very important considering that in a typical porocritical extraction application large and expensive vessels are not used. The reduced complexity of process and its comparative low cost will enable a broader industrial use of CO_2 attributes as a non-toxic and an environmentally benign extraction solvent.

Although, the porocritical extraction is a commercial application, there are only few studies analyzing the mass transfer across the membrane and a physical model to scale-up the process [15,16,19–26].

2.2. Supercritical fluid extraction of metal ions

In this work, the extraction of Cu^{2+} from aqueous solutions using a cation exchanger as extractant was implemented by means of a configuration based on a porocritical extraction process. The membrane contactor operation to remove Cu^{2+} from acid aqueous solutions has been conducted by using 1,1,1-trifluoro-2,4-pentanedione (TFA) or 1,1,1,5,5,5-hexafluoro-2,4-pentanedione (HFA) as extractant compound, since these β-diketones have been previously tested in a dense CO_2 medium [4], considering the favorable kinetics of complex formation, the thermodynamic properties and a comparatively higher extraction capacity of Cu(II) ions reported in the literature [3]. The main characteristics of the extractants used in this work are reported in Fig. 1.

Murphy and Erkey [2,3] developed a thermodynamic model based on combined phase and reaction equilibriums for prediction of the extraction efficiencies by using dense CO_2 with this type of cation exchangers. In this model, the following aqueous phase reactions and three phase equilibrium relations were considered for the extraction of copper:

Aqueous phase reactions:

$$CO_{2(aq)} + H_2O_{(l)} \leftrightarrow H_2CO_{3(aq)} \quad (1)$$

$$H_2CO_{3(aq)} \leftrightarrow HCO_{3(aq)}^{-} + H_{(aq)}^{+} \quad (2)$$

$$HA_{(aq)} \leftrightarrow H_{(aq)}{}^{+} + A_{(aq)}{}^{-} \quad (3)$$

$$2A_{(aq)}{}^{-} + Cu_{(aq)}{}^{2+} \leftrightarrow CuA_{2(aq)} \quad (4)$$

Phase equilibrium relationships:

$$CO_{2(SC)} \overset{K_{CO_2}}{\longleftrightarrow} CO_{2(aq)} \quad (5)$$

$$HA_{(SC)} \overset{K_{HA}}{\longleftrightarrow} HA_{(aq)} \quad (6)$$

$$CuA_{2(SC)} \overset{K_{CuA_2}}{\longleftrightarrow} CuA_{2(aq)} \quad (7)$$

where HA is the cation exchanger and CuA_2 is the complex extracted in the CO_2 phase.

Erkey [5] reported the chemical equilibrium constants for Eqs. (1)–(4) and distribution coefficients (K_{CO_2}, K_{HA}, K_{CuA_2}) of Eqs. (5)–(7). Thus, reactions (1) and (2), and reactions (3) and (4) can be combined as:

$$CO_{2(aq)} + H_2O_{(l)} \overset{K_I = K_1 \cdot K_2}{\longleftrightarrow} H_{(aq)}{}^{+} + HCO_{3(aq)}{}^{-} \quad (8)$$

$$2HA_{(aq)} + Cu_{(aq)}{}^{2+} \overset{K_{II} = K_3^2 \cdot K_4}{\longleftrightarrow} 2H_{(aq)}{}^{+} + CuA_{2(aq)} \quad (9)$$

Erkey [5] reports the equilibrium constants, distribution coefficients as well as the experimental and predicted extraction efficiencies for different chelating agents.

2.3. Experimental

Fig. 2a shows the circulation configuration of solutions inside and outside of the hollow fiber during the experiments. The mass transfer of Cu^{2+} through the membrane was quantified using a single fiber membrane contactor. The liquid feed solution containing Cu^{2+} was circulated into the lumenside, and dense CO_2 phase containing the extractant agents was circulated on the shellside in a countercurrent configuration.

In Fig. 2b the mass transfer of metal ion through the membrane is schematically represented. Concentration profiles of metal ion (M^{z+}), extractant (A) and formed complex ($M(A)_z$) at the proximities of the membrane are represented by dotted lines. A global flow of metal, N_M (mol s^{-1}), is observed from the aqueous solution circulating into the fiber to the dense gas phase circulating in the shellside. The mass transfer of metal at the proximities of the membrane may be described by the integration of the four steps indicated on the figure:

1) Mass transfer of the metal ion (M^{z+}) through the boundary layer of the aqueous feed solution.
2) Mass transfer due to the formation of complex $M(A)_z$ at the interface.
3) Mass transfer of the complex $M(A)_z$ through the membrane pores filled with gas.
4) Mass transfer of the complex through the boundary layer of the extraction solution.

The mass transfer in the first step is represented by the migration of metal ion, M^{z+}, through the boundary layer of the aqueous solution; the second step is the reaction of complex formation at the interface established at the pore mouth. Thus, the global reaction may be represented by the following equation:

$$zHA_{(SC)} + M_{(aq)}{}^{z+} \rightarrow zH_{(aq)}{}^{+} + M(A)_{z(SC)} \quad (10)$$

The third step is represented by the transport of complex $M(A)_z$ into the membrane pores, where the membrane pore is filled with dense gas, and the fourth step is the transport of $M(A)_z$ through the dense gas boundary layer.

An outline of the experimental device used in this work is presented in Fig. 3. Two independent circuits are considered for aqueous feed and extraction streams, which are contacted in the single fiber contactor. The flow rate and pressure of liquid feed solution is controlled by using a HPLC isocratic pump Jasco PU-2080 and the pressure of the CO_2 phase is controlled by ISCO 500D syringe pump with a temperature control jacket connected to a thermostatized bath. The flow rate of the dense CO_2 phase is controlled by means of a micrometering valve AE 10VRMM2812.

In Fig. 3, the black lines represent the aqueous feed solution streams; and the gray ones, the extraction gas streams. In this case, the extractant agent was dissolved in pressurized CO_2. The concentration of extractant in the system was controlled by feeding CO_2 at 52 bar and 20 °C ($\rho_{CO_2} = 152.3$ kg m^{-3}) in a 100 mL view cell (mixture vessel in Fig. 3) containing 3 mL of extractant during 2 h. The initial volume of extractant putted in the mixture vessel was chosen in order to introduce an excess amount of extractant, obtaining a saturation concentration in the CO_2 phase that was injected in the experimental setup. The concentration of extractant in the CO_2 phase has been estimated through the difference between the initial and final mass of extractant contained in the total flow of CO_2 injected to the experimental setup. The extraction phase was circulated at pressures between 70 and 90 bar and 40 °C by using the syringe pump. The extraction solution (CO_2 + β-diketone) circulates through the shellside. A previous theoretical study developed by our group [18] about the mass transfer in porocritical extraction process shows larger values of extraction efficiency when the process is implemented using this configuration.

A single macroporous polytetrafluoroethylene (PTFE) fiber membrane with an outside diameter of 1.8 mm and a wall thickness of 0.4 mm was used to carry out the extraction experiments. The pore size and porosity of the fiber are 2.0 μm and 55%, respectively. Modules with an active length of 0.353 m were prepared potting fibers into a 316L stainless steel shell with an internal diameter of 3.6 mm by means of a solvent-resistant epoxy. The experimental setup described in Fig. 3 is miniaturized hollow fiber contactor system, but this apparatus shows the same fluid dynamic conditions of a pilot or industrial scale system. The process itself does not require conventional solvents and the use of dense CO_2 allows the easy separation of the metal complex formed in the CO_2 phase by means of its depressurization.

On the other hand, the feed solution is an acid $CuSO_4$ solution. Temperature and concentrations of Cu^{2+} were 200 ppm and 40 °C, respectively; pH was ranged between 2.0 and 4.0. These values have been chosen in function of the conditions available in the literature about the thermodynamic and transport properties of the aqueous solutions [5]. The pH values in the aqueous feed solution were adjusted by addition of $H_2SO_{4(aq)}$.

The raffinate obtained from the circulation of liquid solution through the single fiber membrane contactor was collected by means of a micrometering valve (AE 10VRMM2812). The concentration of Cu^{2+} in the raffinate was quantified using a GBC (SensAA) atomic absorption spectrophotometer with a hollow cathode lamp for Copper. The liquid feed solution was circulated with flow rates ranged from 0.1 mL min^{-1} to 1.4 mL min^{-1}, and the dense gas extraction was circulated with a flow rates varying between 1.7×10^{-3} and 3.7×10^{-3} mol min^{-1}.

The transmembrane flux of metal ion (mol m^{-2} h^{-1}) and extraction percentage were calculated from the concentration values of metal ion in the raffinate. Extraction efficiency has been defined by the following equation:

$$EE\,(\%) = \text{Extraction efficiency} = \left(\frac{C_f - C_R}{C_f}\right) \times 100 \quad (11)$$

where C_f is the concentration of metal M in the aqueous feed solution and C_R is the concentration of metal M in the raffinate. Thus, the transmembrane flux of metal ion can be estimated by means

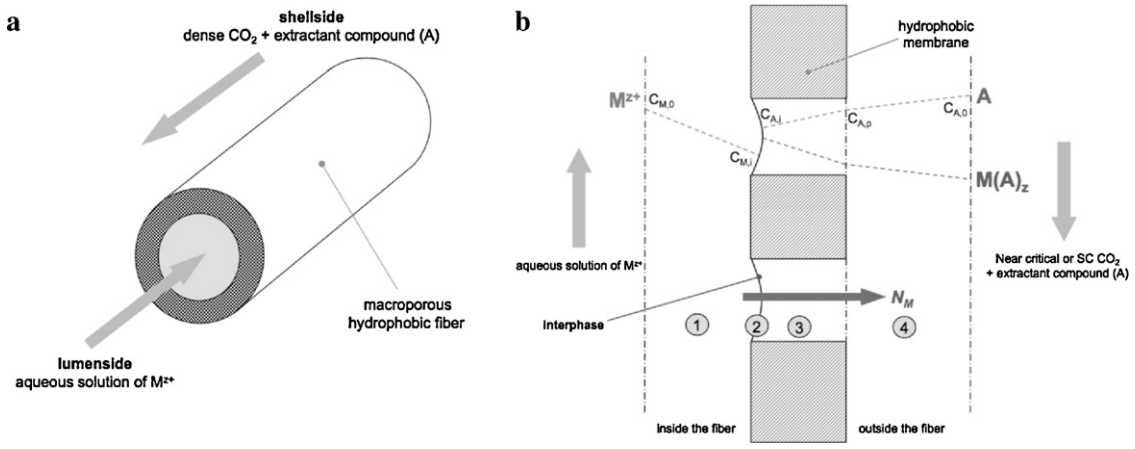

Fig. 2. Outline of the process studied in this work: (a) circulation of the solutions inside and outside the hollow fiber, and (b) schematic representation of the mass transfer of metal ion M^{z+} (Cu^{2+}) through the membrane. The figure shows the concentration profile of the cation M^{z+}, the extractant compound A, and the complex $M(A)_z$ ($Cu(A)_2$) at the proximities of the membrane.

of the mass balance in the membrane contactor according to the following equation:

$$N_M = \left(\frac{F_{aq}(C_f - C_R)}{S_{ID}} \right) \quad (12)$$

where F_{aq} is the aqueous feed solution flow rate and S_{ID} is the surface area available for mass transport on the lumenside. This surface area value was chosen because it corresponds to the surface area of aqueous-dense gas interface, which is considered practically equal to the surface area of the fiber's internal wall.

The mass transfer through the membrane depends on the simultaneous effects of the fluid dynamic conditions in the contactor, the diffusion within the membrane pores and the complex formation kinetics at the interface. In order to evaluate these three aspects, experiments have been carried out to determinate the values of the transmembrane flow and extraction efficiency as a function of the flow rates of solutions, the operating pressure and pH of the aqueous feed solution.

3. Mass transfer model: resistances-in-series approach

3.1. Theoretical considerations and mass transfer equations

Few assumptions and considerations have been taken into account to apply a resistances-in-series approach to describe the overall mass transfer through the membrane, which is controlled by the four steps detailed in Fig. 2. This model was based on the following assumptions: (a) the aqueous feed solution is diluted and hydrodynamic properties are very close to the values for water and its physical properties have been considered constants during the extraction process; (b) the system operates under steady state conditions; (c) reaction is limited at the aqueous-dense gas interface; (d) circulation rates of the solutions in the membrane contactor are under laminar flow conditions.

According to assumptions a, b, and d, the flow of Cu^{2+} (N_M, mol s^{-1}) through the boundary layer of the aqueous solution circulating on the lumenside can be estimated by Eq. (13):

$$N_M^{(1)} = k_1 \cdot S_{ID} \cdot (C_{M,0} - C_{M,i}) \quad (13)$$

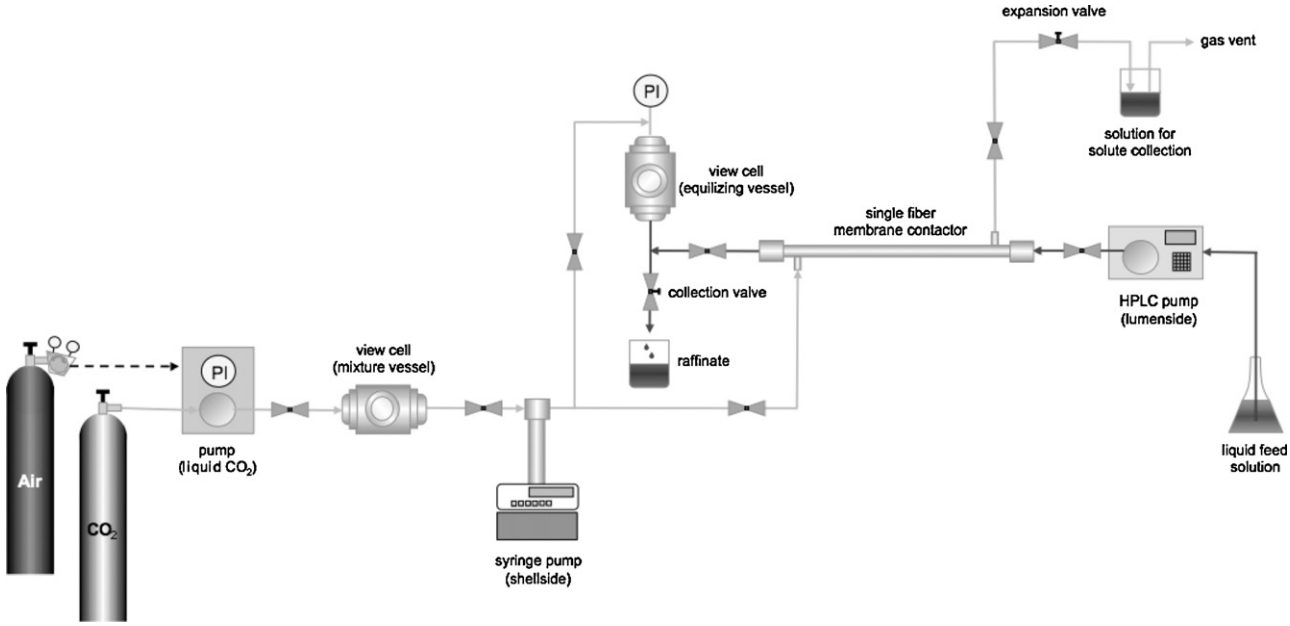

Fig. 3. Outline of the experimental setup based on a single hollow fiber contactor used in this study.

where k_1 is the mass transfer coefficient for the boundary layer of aqueous feed solution at the proximities of the membrane in the lumenside; S_{ID} is the surface area available for mass transport on the lumenside; $C_{M,0}$ is the bulk concentration of Cu^{2+} in the aqueous feed solution and $C_{M,i}$ is its concentration at the interface (see Fig. 2b). The equation of Sieder and Tate [27] may be used to predict the individual mass transfer coefficient into the fiber for the first transfer step when the Reynolds number is lower than 2100:

$$Sh_1 = 1.86\left(Re_1 \cdot Sc_1 \cdot \frac{d_{in}}{L}\right)^{1/3} \quad (14)$$

where Sh_1, Re_1 and Sc_1 are the dimensionless Sherwood, Reynolds and Schmidt numbers, respectively, L is the length of the fiber, and d_{in} is its internal diameter.

In order to fit an effective relationship to estimate the reaction rate of the complex formation at the aqueous-dense gas interface described by Eq. (9), a simple kinetics equation can be proposed:

$$N_M^{(2)} = S_{ID} \cdot k_{eff} \cdot C_{M,i}^{\alpha} \cdot C_{A,i}^{\beta} \cdot C_{H^+,i}^{\gamma} \quad (15)$$

In Eq. (15), $N_M^{(2)}$ represents the overall reaction rate ($mol\,s^{-1}$); $C_{M,i}$ and $C_{A,i}$ are the concentrations of Cu^{2+} and extractant ($mol\,m^{-3}$) at the interface, respectively. Considering the hydrophobic condition of the membrane, the reaction interface would be placed at the pore entrance on the internal side of the fiber. Thus, S_{ID} will be the surface area available for this reaction.

At steady state conditions, the flow of metal ion through the liquid feed phase boundary layer ($N_M^{(1)}$) is equal to the flow of metal ion-TFA complex through the pores. Thus, the flow of complex must be equal to the stoichiometric relationship of the counterflow of TFA from the bulk of the extraction phase to the interface at the pore entrance (N_A), which is represented by the following equation:

$$N_M = -\frac{N_A}{z} \quad (16)$$

In this case, $z = 2$.

If the mass transfer is driven by molecular diffusion, the transfer of extractant TFA in the third transfer step is represented by Eq. (17):

$$N_A^{(3)} = -\frac{\varepsilon \cdot D_{A-CO_2}}{e \cdot \tau} \cdot S_{AV} \cdot (C_{A,p} - C_{A,i}) \quad (17)$$

In this equation, D_{A-CO_2} is the diffusion coefficient of the extractant agent in the dense CO_2 medium; S_{AV} is the average surface area available for mass transport through the membrane pores ($(S_{ID} + S_{OD})/2$); $C_{A,p}$ and $C_{A,i}$ are the concentrations values of TFA at the pore entrance on the shellside and at the interface, respectively (see Fig. 2a); ε, τ and e are the porosity, tortuosity and thickness of the membrane, respectively.

Eqs. (16) and (17) can be combined to estimate the flow of the metal ion in the third transfer step, considering that the transfer of each mol of metal ion M^{z+} through the aqueous solution boundary layer requires z moles of TFA transferred to the interface under steady state conditions. Thus, the molar flow of Cu^{2+} is calculated by Eq. (18). In this study, $z = 2$.

$$N_M^{(3)} = \frac{1}{z}\frac{\varepsilon \cdot D_{A-CO_2}}{e \cdot \tau} \cdot S_{AV} \cdot (C_{A,p} - C_{A,i}) \quad (18)$$

Considering these same assumptions, the flow of metal ion through the dense gas boundary layer in the shellside could be estimated as a function of the TFA transfer by means of the following equation:

$$N_M^{(4)} = \frac{k_4}{z} \cdot S_{OD} \cdot (C_{A,0} - C_{A,p}) \quad (19)$$

where $C_{A,0}$ is the bulk concentration of extractant agent in the extraction phase; S_{OD} is the surface area available for mass transport through the shellside. The mass transfer coefficient, k_4, corresponds to the fourth transfer step indicated in Fig. 2b and it can be calculated by using the correlation proposed by Gawronski and Wrzensika [28] for the shellside when the Reynolds number is lower than 100:

$$Sh_4 = 0.09 \cdot (1 - \phi) \cdot Re_4^{(0.8-0.16\phi)} \cdot Sc_4^{1/3} \quad (20)$$

where ϕ is the packing density of the module and Sh_4, Re_4 and Sc_4 are the dimensionless Sherwood, Reynolds and Schmidt numbers, respectively.

3.2. Determination of chemical kinetics of complex formation

Experimental values of the mass transfer flow of Cu^{2+}, N_M ($mol\,s^{-1}$), have been used to estimate the concentrations of metal ion, $C_{M,i}$, and extractant, $C_{A,i}$, at the liquid–gas interface from Eqs. (13), (18) and (19) under steady state condition ($N_M^{(1)} = N_M^{(2)} = N_M^{(3)}$), since the bulk concentrations of Cu^{2+}, $C_{M,0}$, and extractant, $C_{A,0}$, are known. These concentration values were correlated in order to obtain the parameters k_{eff}, α, β and γ in Eq. (15) applying the method described in a previous work [29] using the LabFit software to predict the transfer of Mo(VI) in a similar membrane extraction process using a organic extraction phase. Thus, an effective chemical kinetics relationship can be obtained to quantify the rate of complex formation at the liquid–dense gas interface. The kinetic model of Eq. (15) obtained from these calculations does not represent the real reaction mechanism at the proximities of the membrane. However, it involves a first approach to extrapolate and scale-up the extraction capacity of the studied system under other fluid dynamic conditions.

3.3. Physical and transport properties of the solutions

Density values of the dense gas extraction phase were obtained from empirical information reported by Reynolds [30] and verified using Peng Robinson EOS. Viscosity of the CO_2 phase was calculated from the method proposed by Lucas [31], while the diffusion coefficient of extractant in dense CO_2 was obtained from data reported by Yang and Matthews [32].

On the other hand, density values of aqueous $CuSO_4$ solutions were obtained from empirical information reported by Klein and Alvarado [33] and its viscosity was calculated from the method proposed by Lucas [31].

Density, viscosity and diffusion coefficient values for both solutions are summarized in Table 1.

4. Results and discussion

4.1. Effect of the fluid dynamics on the Cu(II) extraction performance

In the first part of this study, the effect of the fluid dynamics on the mass transfer rate in the membrane extraction process has been evaluated. In this way, experimental runs according to the procedure described in Section 2.3 were done in order to quantify the extraction percentage of Cu^{2+} as a function of the liquid feed solution and dense CO_2 phase flow rates. From these experiments the mass transfer fluxes ($mol\,h^{-1}\,m^{-2}$) were calculated by means of a mass balance described in Eq. (12). Fig. 4 shows these results for the extraction of Cu^{2+} from aqueous solutions at 90 bar and 40 °C when the liquid feed flow into the lumenside was ranged between 0.1 and 1.0 $mL\,min^{-1}$.

Fig. 4a shows the extraction efficiencies obtained from these experiments, obtaining high extraction values, which are comparable to the solvent extraction process using organic solvents [29,34].

Table 1
Properties of aqueous and CO_2 phases for 70 and 90 bar.

Property	Aqueous phase		Dense phase		Unit
	Pressure: 90 bar	Pressure: 70 bar	Pressure: 90 bar	Pressure: 70 bar	
Density	996.08	995.22	483.81	198.19	$kg\,m^{-3}$
Viscosity	6.645×10^{-4}	6.620×10^{-4}	3.615×10^{-5}	2.017×10^{-5}	$kg\,m^{-1}\,s^{-1}$
Diffusion coefficient	2.695×10^{-9} [a]	2.706×10^{-9}	1.406×10^{-8} [b]	1.489×10^{-8}	$m^2\,s^{-1}$

[a] Diffusion coefficient of Cu^{2+} in water.
[b] Diffusion coefficient of TFA in CO_2.

Higher residence time obtained from lower liquid feed solution flow rates across the hollow fiber contactor increases the extraction efficiency up to 98.7% in this work. The experimental mass transfer fluxes obtained in this study cannot be directly compared to other systems described in the literature, since in our knowledge, there is no previous reports on a similar configuration of membrane-based supercritical fluid extraction of metal ions from aqueous solutions. However, Fig. 4a showed extraction percentages close to 98.7% for the lowest feed solution flow rates, which represent the highest residence times in the membrane contactor (2.78 min). These results represent extraction percentages close to the values reported in literature [5] for supercritical fluid extraction of metal ions in batch configuration, despite these last ones required close to 1 h of operating time.

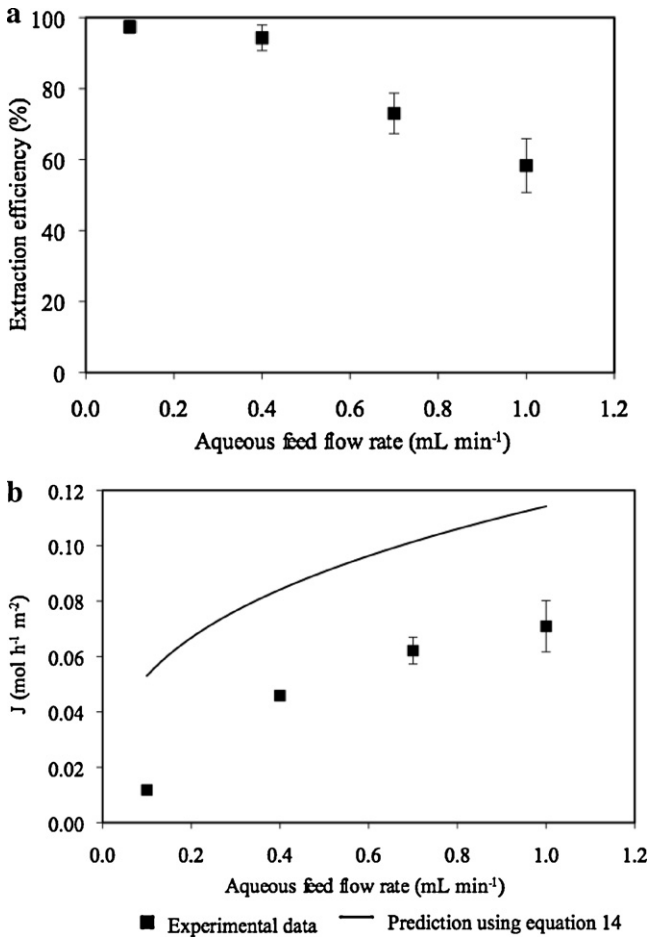

Fig. 4. (a) Extraction efficiency and b) Mass transfer flux values of Cu^{2+} ($mol\,h^{-1}\,m^{-2}$) as a function of the aqueous feed solution flow rate ($mL\,min^{-1}$) at 40 °C and 90 bar. Initial concentration of $CuSO_4$ in the feed phase = 3.147 $mol\,m^{-3}$, pH 2.0. Initial concentration of TFA in the extraction CO_2 phase = 17.716 $mol\,m^{-3}$ in the extraction CO_2 phase, CO_2 phase flow rate = 2.079×10^{-3} $mol\,min^{-1}$.

Moreover, the average solvent/feed mass ratio obtained in this work at 70 and 90 bar was 0.20 and 0.49 kg CO_2/kg of feed solution, respectively. These values could be considered relatively low if they are compared to a typical value of organic/aqueous volumetric ratio near unity in the mixing compartments of liquid–liquid extraction plants [35].

A clear influence of the liquid feed boundary layer on the mass transfer flux may be observed in the Fig. 4a and b. Predictions obtained from Eq. (13) to estimate the Cu^{2+} flux supposing that the concentration of the metal ion is practically equal to zero at the liquid–gas interface in the pore entrance ($C_{M,i}$) are included in Fig. 4b. The theoretical curve obtained from Eq. (13) reports the same behavior of the experimental transfer fluxes in function of the liquid feed flow rate, which proves the significant effect of the liquid feed boundary layer on the overall transfer of Cu^{2+} through the membrane. In this first estimation, both theoretical calculations overestimate experimental data even if they are of the same order of magnitude, but the additional mass transfer resistances (at the membrane pores as well as in the CO_2 phase boundary layer) and the complex formation must be considered for an accurate description of the process. This description is developed in the following sections.

On the other hand, extraction experiments were done for different CO_2 phase flow rate values, which were ranged between 40 and 90 $mL\,min^{-1}$ (measured at 1 atm, 20 °C) and a constant aqueous feed flow rate of 0.7 $mL\,min^{-1}$. Transmembrane Cu(II) flux obtained under these conditions was practically constant with a value of 0.058 ± 0.0054 $mol\,m^{-2}\,h^{-1}$. Fig. 5 shows the transmembrane fluxes of Cu(II) obtained from these experiments. In this case, no significant influence of this variable was observed for the conditions applied in the experiments. This behavior is coherent considering that the liquid feed boundary layer can represent

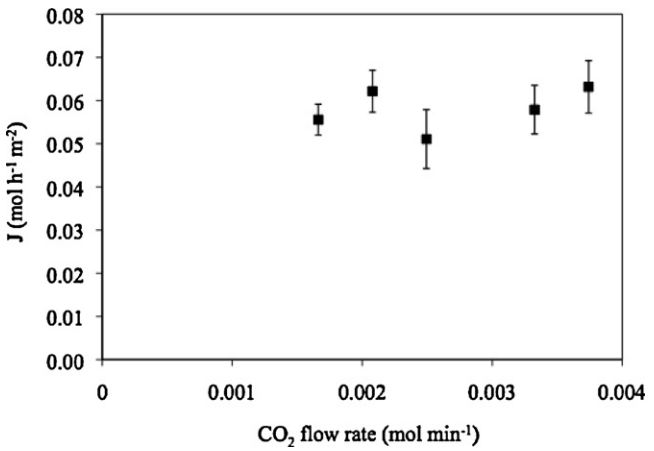

Fig. 5. Experimental values of mass transfer flux of Cu^{2+} ($mol\,h^{-1}\,m^{-2}$) as a function of the CO_2 phase flow rate at 40 °C and 90 bar. Initial concentration of $CuSO_4$ in the feed phase = 3.147 $mol\,m^{-3}$, pH 2.0, initial concentration of TFA in the extraction CO_2 phase = 17.716 $mol\,m^{-3}$, aqueous feed flow rate = 0.7 $mL\,min^{-1}$.

an important fraction of the overall mass transfer resistances and the complex formation kinetic at the liquid–gas interface and the complex transport through the membrane pores could represent significant barriers on the mass transfer rate through the membrane.

4.2. Chemical aspects of the extraction mechanism: the effect of the extractant compound and pH

Extraction experiments of Cu^{2+} were carried out as a function of liquid feed flow rate for two different extractant compounds. These extractants were two different β-diketones: 1,1,1-trifluoro-2,4-pentanedione (TFA) and 1,1,1,5,5,5-hexafluoro-2,4-pentanedione (HFA), which were used considering the experimental data reported in the literature about its high solubility in pressurized CO_2 and low solubility in water as well as its application in Cu(II) extraction experiments [36,37]. Previous to the extraction experiments, β-diketones were dissolved in CO_2 at 50 bar and 25 °C in a view cell before to be injected in the extraction device. Thus, similar mass of diketones was injected in the extraction system for each experimental run. From this procedure, the concentration of TFA and HFA in the dense CO_2 phase before the extraction process was 17.7 mol m^{-3} and 18.4 mol m^{-3}, respectively. Thus, similar concentrations allow the same stoichiometric availability for the complex formation.

TFA seems to be a better extractant compound than HFA. Fig. 6a and b reports the extraction efficiencies and transmembrane fluxes obtained from different experimental runs with both extractants. The best extraction capacity of TFA could be related with the structure of both diketones compounds. The difference is the number and position of fluorine atoms. TFA poses three fluorine atoms located in the same carbon atom in one extreme of its structure whereas HFA has six fluorine atoms positioned in the opposite extreme of the molecule. It is well known that fluorine atom is clearly electronegative attracting electrons and generating a positive pole in other atom of the compound. Diketones as extractants act as cationic exchanger since due a tautomeric equilibrium, which originate around their structures an enolic isomer with an hydroxyl group which provides the acid hydrogen-ion which is exchangeable by a metallic ion, the Cu(II) ions in this study. In the case of TFA, the three fluorine atoms attract electrons towards its position facilitating the keto-enol tautomerism around the carbon atom neighbor generating the OH^- group with the acid proton used in the cation exchange equilibrium with Cu(II). In turn, HFA structure with three fluorine atoms in opposite extreme of its structure bring about the annulment of this fact because all F^- atoms tend to attract electrons towards their opposite side preventing the keto-enol tautomeric equilibrium and making difficult the formation of hydroxyl-group with the acid-proton. In the HFA extractant molecule, it is not possible the occurrence of a kind of a double keto-enol tautomeric equilibrium to each side of the molecule since would require two double-bonds in a same central carbon atom. Two double bonds are possible in a conjugate structure as in the aromatic-ring containing compounds.

In Fig. 6a is clear that a higher aqueous flow rate decreases the residence time of the copper-containing solution inside the reactor, which avoid obtaining higher equilibrium concentration of metal complex in the CO_2 phase.

On the other hand, Fig. 6b reports that higher aqueous feed flow rate values involve higher metal fluxes through the membrane, which show that the overall transport rate could be determined by the chemical kinetic step, since a greater concentration of copper ions available at the reaction interface would be increasing the complex formation rate.

On the other hand, a significant effect of the pH of the liquid feed solution can be observed from different extraction experiment

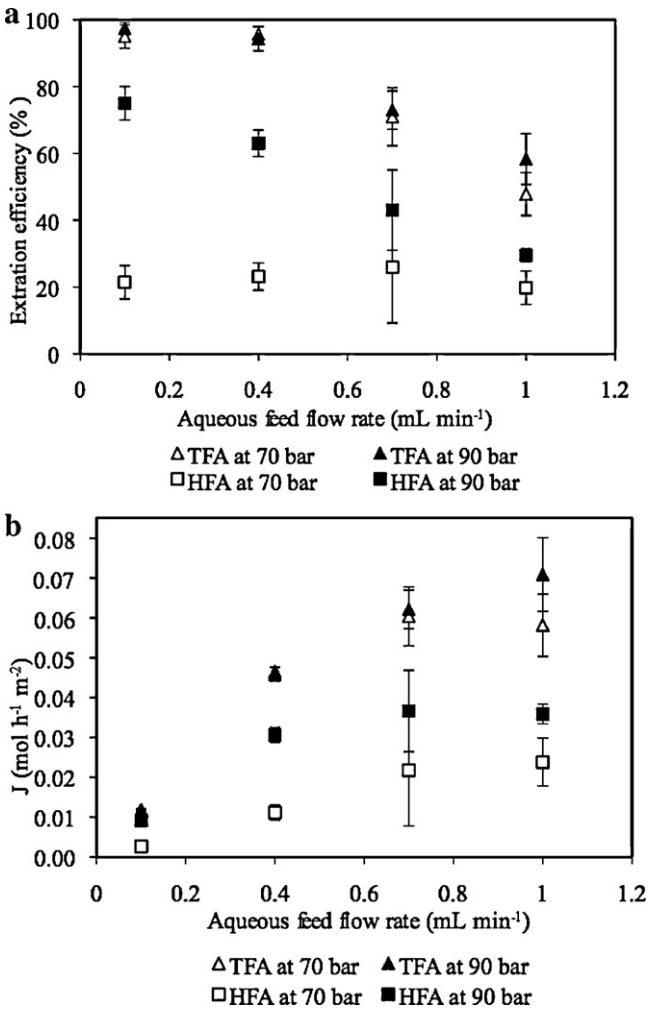

Fig. 6. (a) Extraction efficiency and (b) mass transfer flux values of Cu^{2+} (mol h^{-1} m^{-2}) as a function of the aqueous feed solution flow rate (mL min^{-1}) and type of extract agent at 40 °C and 90 bar. Initial concentration of $CuSO_4$ in the feed phase = 3.147 mol m^{-3}, pH 2.0, initial concentration of TFA in the extraction CO_2 phase = 17.716 mol m^{-3} and HFA in the extraction CO_2 phase = 18.37 mol m^{-3}, CO_2 phase flow rate = 2.079×10^{-3} mol min^{-1}.

done under the same operation conditions. Fig. 7 shows that the extraction efficiency at pH 2.0 is 3.5 times higher than the obtained one at pH 4.0. Chou and Yang [38] suggest that the pH of the solution should be a critical parameter in the extraction efficiency of indium(III) ions using a β-diketone (AcAcH) as extractant compound. A previous study [39] showed that when water is in contact with supercritical CO_2, the pH value at the equilibrium is less than 3.0 due to the formation and dissociation of an important amount of carbonic acid in water. Therefore, the optimum pH values for dense CO_2 extraction should be ranged from 2.0 to 3.0.

The influence of the acidity of the aqueous solution on the extraction performance showed in Fig. 7a and b would confirm that is required a high content of protons (lower pH values) to facilitate and stabilize the formation of the keto-enol tautomerism. A higher pH could revert the equilibrium towards the keto-form, which clearly has lower extraction capacity.

In this work, the maximum operation pressure was 90 bar and the highest extraction efficiencies (98.7%) were obtained at pH 2.0. Under these conditions, corrosion was not observed in the experimental setup during the 18 weeks spent to achieve these experimental runs.

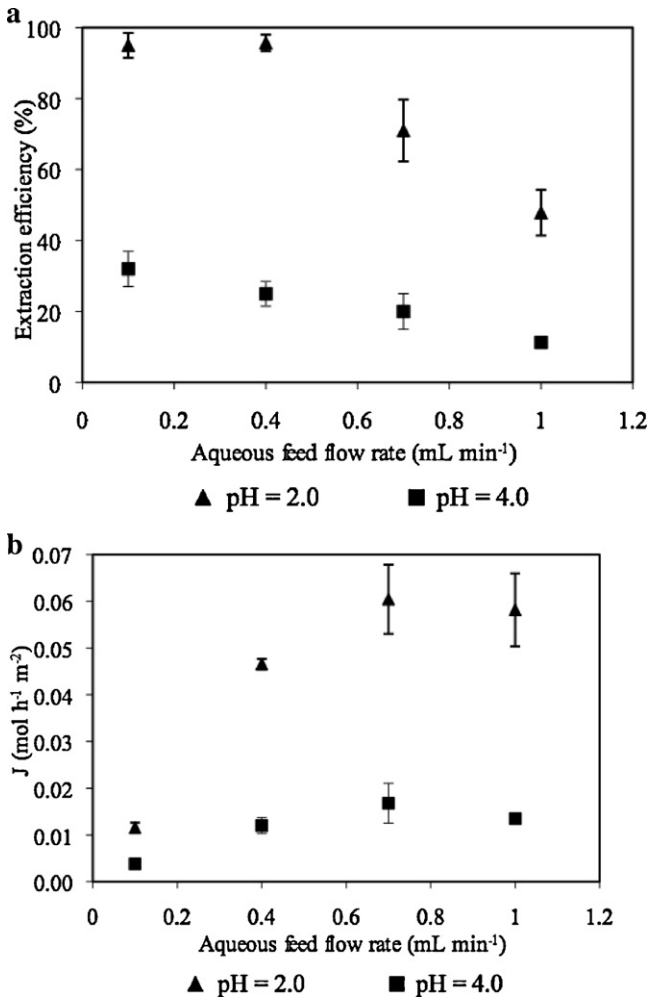

Fig. 7. (a) Extraction efficiency and (b) mass transfer flux values of Cu^{2+} ($mol\,h^{-1}\,m^{-2}$) as a function of the aqueous feed solution flow rate ($mL\,min^{-1}$) for different pH values at 70 bar. Initial concentration of $CuSO_4$ in the feed phase = 3.147 $mol\,m^{-3}$. Initial concentration of TFA in the extraction CO_2 phase = 17.716 $mol\,m^{-3}$, CO_2 phase flow rate = 2.079×10^{-3} $mol\,min^{-1}$.

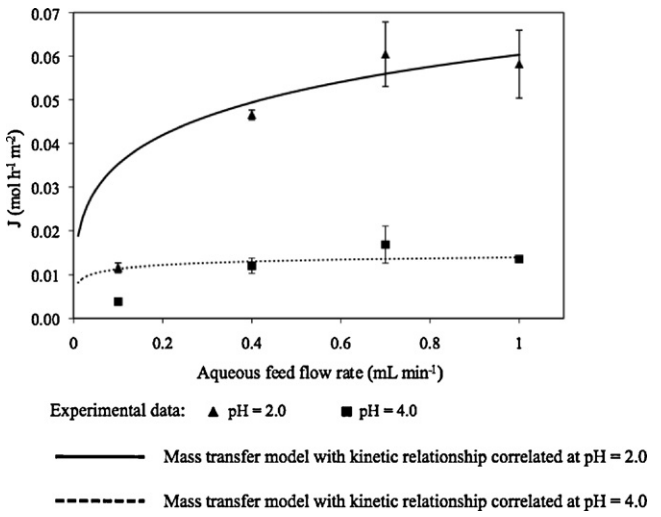

Fig. 8. Experimental data of metal ion (Cu^{2+}) transfer flux as a function of the aqueous feed flow rate for different pH values and its prediction using the mass transfer model proposed in this work. Operating pressure = 70 bar; initial concentration of $CuSO_4$ in the feed phase = 3.147 $mol\,m^{-3}$; initial concentration of TFA in the extraction CO_2 phase = 17.716 $mol\,m^{-3}$ and CO_2 phase flow rate = 2.079×10^{-3} $mol\,min^{-1}$.

4.3. Influence of the pressure on the mass transfer rate

The operation pressure should be an important variable on the extraction efficiency, since the pressure can have a significant influence on the solubility of β-diketones and its metal complexes in the CO_2 phase, as well as the availability of dissolved CO_2 and the pH in the aqueous phase. Fig. 6 shows the effect of the pressure value on the extraction efficiency and transmembrane flux of Cu(II) ions obtained from experiments as a function of the liquid feed flow rate and two different extractants.

It is possible to observe that the pressure increasing from 70 to 90 bar improves the extraction efficiency in all the cases. However, the magnitude of this improvement is different depending on the extractant compound. The results reported in Fig. 6 consider similar concentration ($mol\,m^{-3}$) for both extractants (TFA and HFA) in the CO_2 phase that is fed in the extraction system. Higher extraction efficiencies were obtained using TFA, which has a chemical structure favorable to the cationic exchange mechanism explained in Section 4.2.

On the other hand, the increasing of pressure in the extraction experiments represents a significant density increase in the CO_2 phase, from 198.2 $kg\,m^{-3}$ at 70 bar to 483.8 $kg\,m^{-3}$ at 90 bar. The density increase can be associated to an important increasing of the complex solubility in the CO_2 phase, which can explain the large improvement of the extraction efficiency when HFA was used at 90 bar.

The effect of the pressure on the extraction efficiency and the mass transfer flux could be explained by the solubility on CO_2 and the subsequent availability of carbonic acid in the aqueous phase. Fig. 7 shows that the extraction efficiency and the mass transfer rate are improved at lower pH values. The pH reported in this figure represent its initial value in the feed aqueous solution circulated through the membrane contactor. The real pH value in the aqueous phase during the extraction process could have decreased due to the solubility of pressurized CO_2. Thus, the effect of pH and pressure could be coupled. In this case, the extraction mechanism and physicochemical nature of CO_2 generate a coupled effect of pressure and pH value on the mass transfer rate.

4.4. Phenomenological approach for determination of complex formation kinetic

From the phenomenological Eqs. (13), (18) and (19) as well as the experimental metal ion transfer flow values (N_M), the interfacial concentrations of Cu^{2+}, $C_{M,i}$, and extractant, $C_{A,i}$, were directly estimated in order to correlate the parameters of Eq. (15). The concentration of protons at the interface, $C_{H^+,i}$, can be considered much higher than the metal ion and the extractant ones and its value will be similar to bulk concentration. Thus, Eq. (15) represents the effective complex formation rate at the interface as a function of the concentrations of Cu^{2+}, extractant and protons.

Several simple partial orders of reaction α, β and γ were tested using LabFit. The best correlation was obtained when reaction orders respect to Cu^{2+} (α), extractant (β) and protons (γ) in Eq. (15) were 2.0, 1.0 and 0.642, respectively. k_{eff} is the effective kinetic constant of the complex formation and its value was estimated in 1.4313×10^{-7} ($mol^{2.642}\,m^{8.926}\,s^{-1}$).

Fig. 8 shows the experimental transmembrane Cu ions fluxes ($mol\,m^{-2}\,h^{-1}$) compared to the values obtained by the correlated model. Good agreement between the model and experimental data is expected except for predictions at very low aqueous feed solution flow rate. This could be explained by limited prediction capacity of the effective reaction equation or an inaccurate prediction of the mass transfer coefficients at the proximities of the membrane when flow rates or Reynolds number are very low. The Reynolds

Table 2
Contribution of local transfer steps to the global mass transfer resistance. Results obtained from experimental data obtained at 40 °C and 70 bar. Initial concentration of $CuSO_4$ in the feed phase = 3.147 mol m^{-3}; initial concentration of TFA in the extraction CO_2 phase = 17.716 mol m^{-3} and CO_2 phase flow rate = 2.0785 × 10^{-3} mol min^{-1}.

pH	Feed flow rate (mL min^{-1})	Resistance			
		Contribution of the aqueous feed boundary layer (%)	Contribution of kinetic of the complex formation (%)	Contribution of the gas gap in the membrane pores (%)	Contribution of the CO_2 phase boundary layer (%)
2.0	0.1	46.29	6.67	5.26	41.77
	0.4	35.19	8.05	6.35	50.41
	0.7	31.06	8.57	6.76	53.62
	1.0	28.57	8.87	7.00	55.55
4.0	0.1	20.88	57.90	2.37	18.84
	0.4	14.26	62.75	2.57	20.42
	0.7	12.13	64.31	2.64	20.93
	1.0	10.91	65.19	2.67	21.22

number into the lumenside of the single fiber contactor is lower than 6.5 when the aqueous feed solution flow rate is lower than 0.2 mL min^{-1}.

4.5. Assessment of the local mass transfer resistances

The relevance of every local transport resistances can be quantified from the mass transfer model coupled to the complex formation rate equation. In a previous work, Valdés and coworkers [29] estimated the contributions of different mass transfer steps on the basis in the local transport resistances for the boundary layers, membrane pores and reaction rate in the membrane-based solvent extraction of Mo(VI). According to the resistances-in-series model, the rate-controlling steps can be identified by means of the quantification of the fractional resistances. These calculations can be adapted to the system studied in this work, since it represents the same process configuration. Table 2 summarizes the fractional transfer resistances for each contribution as a function of pH and aqueous feed flow rate.

From the results reported in Table 2 two mass transfer behaviors influencing the extraction process can be observed. When the pH value of the aqueous solution is 2.0 fractional mass transfer resistances are concentrated on the boundary layers at the proximities of the membrane. The effect of the complex formation rate and the complex transfer through the membrane pores can be considered not significant on the overall resistance. Thus, Fig. 4b shows the theoretical curve of transmembrane metal ion flux predicted by means of Eq. (13) when pH is 2.0, supposing that the concentration of Cu^{2+} at the aqueous-CO_2 interface, $C_{M,i}$, is equal to cero. The predicted flux value represents the maximum value that could be observed through the aqueous feed boundary layer.

On the other hand, when pH value is 4.0 fractional mass transfer resistances of boundary layers continue contributing more than 30% of the overall resistance. However, the complex formation rate increases its contribution, becoming the rate-controlling step of this process. The reaction rate can represent 65.19% of the overall mass transfer resistance under this condition.

5. Conclusions

In this work, dense gas extraction of Cu^{2+} from aqueous solutions has been implemented in a continuous configuration using a hydrophobic hollow fiber contactor. The extraction phase was pressurized CO_2 containing β-diketones. High extraction efficiency up to 98.7% can be obtained under steady state operation. The mass transfer fluxes through the membrane seems to be higher than similar membrane-based extraction processes reported in the literature using organic solvents, since transport properties of the extraction phase are closer to the gas phase. However, the response of the studied system to the operation variables related to chemical aspects such as pH, pressure and structure of the extractant compound are different from what is usually expected in solvent extraction using cation exchangers. In this way, the influence of the acidity of the aqueous solution on the extraction performance could confirm that is required a high content of protons to facilitate and stabilize the formation of a keto-enol tautomerism during the complex formation. The effect of pH and pressure may be coupled in the reaction mechanism, since the solubility of CO_2 in the aqueous phase could modify the initial content of protons in the aqueous solution.

From the experimental results and phenomenological equations an effective complex formation rate was estimated at the aqueous-CO_2 interface. This effective kinetic equation allows correlating the transfer of Cu^{2+} through the porous membrane and it could be used as a tool to scale-up this process. Nevertheless, this kinetic model is not useful to understand the real mechanism of the complex formation. Thus, the fit of correlated data is poor at low circulation rates when the complex formation reaction is highly influenced by the transfer of reactants from the bulk of both phases to the proximities of the membrane. Future researches should be focused on the introduction of the mechanistic aspects in the transfer model in order to improve its prediction capacity and the design of new intensified extraction processes for other metal ions or hazardous materials.

Acknowledgments

This research has been developed in the framework of the Projects FONDECYT 1100305 (CONICYT Chile) and ECOS-CONICYT C10E05. The financial support for the PhD student Hugo Valdés is gratefully acknowledged.

References

[1] S.M. Walas, Phase Equilibria in Chemical Engineering, Butterworth-Heinemann, Boston, 1985.
[2] J. Murphy, C. Erkey, Copper(II) removal from aqueous solutions by chelation in supercritical carbon dioxide using fluorinated β-diketones, Industrial and Engineering Chemistry Research 36 (1997) 5371.
[3] J. Murphy, C. Erkey, Thermodynamics of extraction of copper(II) from aqueous solutions by chelation in supercritical carbon dioxide, Environmental Science & Technology 31 (1997) 1674.
[4] K. Laintz, C. Hale, P. Stark, C. Rouquette, J. Wilkinson, A comparison of liquid and supercritical carbon dioxide as an extraction solvent for plating bath treatment, Analytical Chemistry 70 (1998) 400–404.
[5] C. Erkey, Supercritical carbon dioxide extraction of metal ions from aqueous solutions: a review, Journal of Supercritical Fluids 17 (2000) 259–287.
[6] K. Soldenhoff, M. Shamieh, A. Manis, Liquid–liquid extraction of cobalt with hollow fiber contactor, Journal of Membrane Science 252 (2005) 183–194.
[7] Y.J. Wang, Y. Wang, F. Chen, G.S. Luo, Y.Y. Dai, Mass transfer characteristics of cadmium(II) extraction in hollow fiber modules, Chemical Engineering Science 58 (2003) 3223–3231.
[8] R.S. Juang, H.C. Kao, Extraction separation of Co(II)/Ni(II) from concentrated HCl solutions in rotating disc and hollow-fiber membrane contactors, Separation and Purification Technology 42 (2005) 65–73.

[9] F.J. Alguacil, Facilitated transport and separation of manganese and cobalt by a supported liquid membrane using DP-8R as a mobile carrier, Hydrometallurgy 65 (2002) 9–14.
[10] F. Valenzuela, M. Vega, M. Yáñez, C. Basualto, Application of a mathematical model for copper permation from a Chilean mine water through a hollow fiber-type supported liquid membrane, Journal of Membrane Science 204 (2002) 385–400.
[11] A. Gabelman, S. Hwang, Hollow fiber membrane contactors, Journal of Membrane Science 159 (1999) 61–106.
[12] J.G. Crespo, I.M. Coelhoso, R.M.C. Viegas, Membrane contactors: membrane separations, in: Encyclopedia of Separation Science, 2000, pp. 3303–3311.
[13] K. Sirkar, Membrane separation technologies: current developments, Chemical Engineering Communications 157 (1997) 145–184.
[14] J. Robinson, M. Sims, Method and system for extracting a solute from a fluid using dense gas and a porous membrane, U.S. Patent 5,490,884, 1996.
[15] M. Sims, Porocritical fluid extraction from liquids using near-critical fluids, Membrane Technology 97 (1998) 11–12.
[16] S. Bocquet, J. Romero, J. Sanchez, G. Rios, Membrane contactors for the extraction process with subcritical carbon dioxide or propane: simulation of the influence of operating parameters, Journal of Supercritical Fluids 41 (2) (2007) 246–256.
[17] H. Estay, Modeling and simulation of the mass transfer and selectivity of membrane contactor systems using supercritical fluids. Master Thesis, Chemical Engineering, University of Santiago de Chile, 2005.
[18] H. Estay, S. Bocquet, J. Romero, J. Sanchez, G. Rios, F. Valenzuela, Modeling and simulation of mass transfer in near-critical extraction using a hollow fiber membrane contactor, Chemical Engineering Science 62 (21) (2007) 5794–5808.
[19] G. Bothun, B. Knutson, H. Strobel, S. Nokes, E. Brignole, S. Díaz, Compressed solvents for the extraction of fermentation products within a hollow fiber membrane contactor, Journal of Supercritical Fluids 25 (2003) 119–134.
[20] M. Sims, E. McGovern, J. Robinson, Porocritical fluid extraction application: continuous pilot extraction of natural products from liquids with near-critical fluids, in: Proceeding of 5th Meeting on Supercritical Fluids, Materials and Natural Processing, Nice, France, 1998.
[21] M. Sims, E. Estigarribia, Continuous sterilization of aqueous pumpable food using high pressure carbon dioxide, in: 4th International Symposium on High Pressure Process Technology and Chemical Engineering, Venice, Italy, 2002, pp. 22–25.
[22] M. Sims, E. Estigarribia, Membrane carbon dioxide sterilization of liquid food: scale up of a commercial continuous process, in: 6th International Symposium on Supercritical Fluids, Versailles, France, 2003, pp. 28–30.
[23] M. Sims, Simultaneous reaction and extraction with near-critical carbon dioxide using a membrane contactor, in: International Symposium on Supercritical Fluids, ISSF 2005, Orlando, USA, 2005, pp. 1–4.
[24] S. Bocquet, A. Torres, J. Sanchez, G. Rios, J. Romero, Modeling the mass transfer in solvent-extraction processes with hollow-fiber membranes, AIChE Journal 51 (2005) 1067–1079.
[25] A. Gabelman, S. Hwang, Experimental results versus model predictions for dense gas extraction using a hollow fiber membrane contactor, Journal of Supercritical Fluids 35 (2005) 26–39.
[26] A. Gabelman, S. Hwang, A theoretical study of dense gas extraction using hollow fiber membrane contactor, Journal of Supercritical Fluids 37 (2006) 157–172.
[27] R. Bird, W. Stewart, E. Lightfoot, Fenómenos de Transporte, 1st ed., Reverté S.A., México, 1998.
[28] R. Gawronski, B. Wrzesinska, Kinetics of solvent extraction in hollow fiber contactors, Journal of Membrane Science 168 (2000) 213–222.
[29] H. Valdés, J. Romero, J. Sanchez, S. Bocquet, G. Rios, F. Valenzuela, Characterization of chemical kinetics in membrane-based liquid–liquid extraction of molybdenum(VI) from aqueous solutions, Chemical Engineering Journal 151 (1–3) (2009) 333–341.
[30] W. Reynolds, Thermodynamic Properties in SI: Graphs, Tables and Computational Equations for Forty Substances, Department of Mechanical Engineering, Stanford University, Stanford, CA, 1979.
[31] B. Poling, J. Prausnitz, J. O'Connell, The Properties of Gases and Liquids, 5th ed., McGraw Hill, 2001.
[32] X. Yang, M. Matthews, Diffusion of chelating agents in supercritical CO_2 and a predictive approach for diffusion coefficients, Journal of Chemical and Engineering Data 46 (2001) 588–595.
[33] Y. Çengel, M. Boles, Thermodynamics, McGraw Hill, 2006.
[34] F. Valenzuela, C. Basualto, C. Tapia, J. Sapag, C. Paratori, Recovery of copper from leaching residual solutions by means of a hollow fiber membrane extractor, Minerals Engineering 9 (1) (1996) 15–22.
[35] K.C. Sole, Solvent extraction in the hydrometallurgical processing and purification of metals: process design and selected applications, in: M. Aguilar, J.M. Cortina (Eds.), Solvent Extraction and Liquid Membranes: Fundamentals and Applications in New Materials, CRC Press, Boca Raton, 2008, pp. 141–200.
[36] W. Cross, A. Akgerman, C. Erkey, Determination of metal-chelate complex solubilities in supercritical carbon dioxide, Industrial and Engineering Chemistry Research 35 (1996) 1765–1770.
[37] R. Gupta, J. Shim, Solubility in Supercritical Carbon Dioxide, Taylor & Francis Group, LLC, 2007.
[38] W. Chou, K. Yang, Effect of various chelating agents on supercritical carbon dioxide extraction of indium(III) ions from acidic aqueous solution, Journal of Hazardous Materials 154 (1–3) (2008) 498–505.
[39] K. Toews, R. Shroll, C. Wai, N. Smart, pH-defining equilibrium between water and supercritical CO_2. Influence on SFE of organics and metal chelates, Analytical Chemistry 67 (1995) 4040–4043.